

Celler: A Genomic Language Model for Long-Tailed Single-Cell Annotation

Huan Zhao^{1*}, Yiming Liu^{1,2}, Jina Yao^{1,2}, Ling Xiong^{1,2}, Zexin Zhou^{1,2}, Zixing Zhang^{1*}

¹School of Computer Science and Electronic Engineering, Hunan University, Changsha 410082, China
²Higentec AiLab

{hzhao@hnu.edu.cn, zixingzhang@hnu.edu.cn}

Abstract

Recent breakthroughs in single-cell technology have ushered in unparalleled opportunities to decode the molecular intricacy of intricate biological systems, especially those linked to diseases unique to humans. However, these progressions have also ushered in novel obstacles—specifically, the efficient annotation of extensive, long-tailed single-cell data pertaining to disease conditions. To effectively surmount this challenge, we introduce Celler, a state-of-the-art generative pre-training model crafted specifically for the annotation of single-cell data. Celler incorporates two groundbreaking elements: First, we introduced the Gaussian Inflation (GInf) Loss function. By dynamically adjusting sample weights, GInf Loss significantly enhances the model’s ability to learn from rare categories while reducing the risk of overfitting for common categories. Secondly, we introduce an innovative Hard Data Mining (HDM) strategy into the training process, specifically targeting the challenging-to-learn minority data samples, which significantly improved the model’s predictive accuracy. Additionally, to further advance research in this field, we have constructed a large-scale single-cell dataset: Cell-75, which encompasses 40 million cells distributed across 80 human tissues and 75 specific diseases. This dataset provides critical support for comprehensively exploring the potential of single-cell technology in disease research. Our code is available at <https://github.com/AI4science-ym/HiCeller>.

1 Introduction

Single-cell RNA sequencing (scRNA-seq) is a technique that reveals differences in gene expression and cellular functional heterogeneity among different cells by studying intracellular transcript (mRNA) expression at the single-cell level [Grabski and Irizarry, 2022]. The rapid development of single-cell RNA sequencing (scRNA-seq) technology has greatly improved our understanding of cellular heterogeneity and disease mechanisms [Lukassen *et al.*, 2020; He *et al.*, 2020;

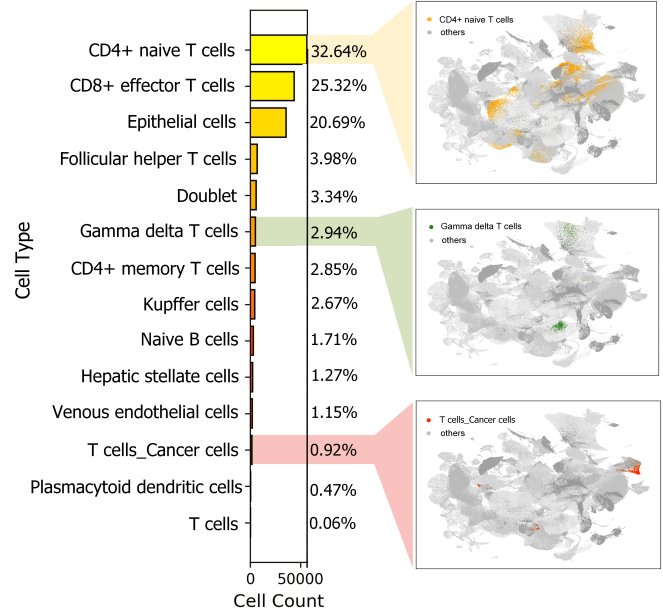


Figure 1: Long-Tail Data Distribution

McDavid *et al.*, 2013], making it possible to accurately characterize different cell types at the single-cell level [Plass *et al.*, 2018; Cao *et al.*, 2019; Schaum *et al.*, 2018; Zhao *et al.*, 2020; Pliner *et al.*, 2019]. Compared with traditional cluster-level transcriptome sequencing, single-cell transcriptome sequencing provides more accurate gene expression information for each cell, thus solving the problem of averaging effect due to cell mixing in cluster-level sequencing [Huang *et al.*, 2021; Tarashansky *et al.*, 2021]. However, the explosion in the amount of single-cell data also poses significant challenges, especially in data annotation. When dealing with large-scale data, traditional manual annotation methods are not only time-consuming and labour-intensive due to their reliance on manual operations, but also the manual methods are particularly cumbersome and error-prone.

Due to the high dimensionality of mRNA data, traditional machine learning methods are typically limited to capturing linear features during the dimensionality reduction process, making it challenging to account for the intrinsic associations within RNA expression data and the nonlinear expression characteristics across different cells [Pasquini *et al.*, 2021]. To address this limitation, researchers in re-

cent years have introduced large language models, aligning the conceptual framework of transcriptomic data with that of natural language data [Ganin and Lempitsky, 2015; Zhang *et al.*, 2010]. For example, some state-of-the-art genomic language models (GLMs), such as scBERT [Yang *et al.*, 2022], scGPT [Cui *et al.*, 2023], CellPLM [Wen *et al.*, 2023], Geneformer [Theodoris *et al.*, 2023] and tGPT [Shen *et al.*, 2023], are specifically designed for single-cell data designed as pre-trained models. These models treat genes as tokens (words), randomly mask some non-zero gene expression values and make predictions based on the remaining data, thus effectively capturing complex relationships between genes and improving cell representation.

Nevertheless, the methods outlined earlier exhibit certain limitations in deeply deciphering the molecular mechanisms of these diseases. This is mainly due to the fact that the number of disease-related cells is typically vastly outnumbered by normal tissue cells, causing the data to exhibit marked long-tail distribution characteristics. This is particularly pronounced in the investigation of complex diseases such as cancer, where certain pivotal cells or genes may be underrepresented, impeding the model’s ability to effectively apprehend critical information. As shown in Figure 1, in the cell appearance of the lung organ of a patient with lung cancer, the proportion of lung cancer cells is only 0.92%. In this case, the attention to diseased cells in the above model training may be diluted by a large number of normal cells, thereby weakening the recognition ability of these key cells, and even possibly distorting our understanding of disease mechanisms.

To address this issue, we propose Gaussian Inflation (GInf) Loss, a loss function specifically designed for long-tailed data, which aims to enhance the model’s sensitivity to rare categories. GInf Loss dynamically increases the feature weights of individual data instances from tail categories in a Gaussian distribution pattern, based on the size of the category data in the dynamic space. This approach benignly adjusts the balance between positive and negative sample weights in the feature space, effectively mitigating the model’s learning deficiencies in handling rare cell types. As a result, the network is better able to focus on diseased cells and their associated genes.

In addition, we propose a Hard Data Mining (HDM) training strategy for difficult sample mining. This strategy utilizes the model’s final output classification confidence as an evaluation metric, defining misclassified samples with high confidence as difficult samples. During training, additional attention is given to these difficult samples by increasing their training iterations, thereby enhancing the overall accuracy of the model.

In the course of our in-depth exploration in this field, we have not only proposed novel methods but also constructed a large-scale private dataset, Celler-75. This dataset boasts an unparalleled volume, comprising 40 million annotated cell samples, covering 80 types of human tissues and 75 specific diseases. To the best of our knowledge, the scale, depth, and breadth of this dataset far surpass any publicly available datasets at present. For instance, when compared to public datasets such as Multiple Sclerosis (MS) [Schirmer *et al.*, 2019] and human pancreas (hPancreas) [Chen *et al.*,

2023], the difference in data volume becomes evident. The MS dataset contains only 13,468 cell samples in its training set and 7,000 in its test set. Similarly, the hPancreas dataset includes only 10,600 cell samples in its training set and just 4,218 in its test set.

Overall, our contributions are listed below:

- We have developed the largest known single-cell dataset based on human disease tissues, which includes 75 types of human diseases, containing over 40 million cells and over 9 million genes.
- We introduced GInf Loss to address the long-tail distribution in disease data, enabling the model to focus on rare disease cell types and specific genes.
- By introducing the Hard Data Mining (HDM) training strategy, the overall performance of the model has been improved.

2 Related works

2.1 Genomic Language Model

This work focus on applying large-scale model technology in the single-cell domain, expanding sc-RNAseq data, and designing experiments to achieve cell annotation.

A notable contribution in this field is scBERT [Yang *et al.*, 2022], which employs a multi-layer Performer to pre-train scRNAseq data, followed by fine-tuning to adapt to various downstream tasks. Building on this foundation, the work by xTrimoGene [Gong *et al.*, 2023] enhanced scBERT with two key improvements: pruning zero-expression genes and refining the expression binning strategy through automatic discretization. These modifications significantly boosted the model’s scalability and feature resolution. The latest preprint, scGPT [Cui *et al.*, 2023], introduced a variant of masked language modeling that mimics autoregressive generation in natural language processing, iteratively predicting masked genes based on the model’s confidence. In contrast, CellPLM [Wen *et al.*, 2023] proposes a pretraining method for cell language models that goes beyond single cells. CellPLM not only captures the gene expression patterns within individual cells but also considers the interactions between cells and the tissue structure, thereby providing a more comprehensive understanding of cellular functions. These innovative approaches open new avenues for single-cell omics research, advancing our understanding of cellular functions.

2.2 Long-Tail for Classification

Resampling and Reweighting In the real world, data often follow a long-tailed distribution, which can pose challenges to the classifier. To mitigate data imbalance, directly under or up sampling [Chawla *et al.*, 2002; He and Garcia, 2009; Zhong *et al.*, 2016; Buda *et al.*, 2018] the training instance based on the relation of class size is a straightforward method which drives us to repeat the learning tail instance and ignore the learning of head classes. Reweighting assigns loss functions to the sample of different class and adjusts the effect of label frequency on the loss function.

Integrated Learning Ensemble learning methods have demonstrated outstanding performance in addressing long-tailed classification tasks. Researchers leverage individual

expert modules to capture the distribution characteristics of different data groups, subsequently combining the learning outcomes from each expert module. During the training phase, these expert modules operate independently, avoiding mutual interference and enabling focused and efficient learning. Expert-based ensemble strategies, such as BBN [Zhou *et al.*, 2020] and RIDE [Zhang *et al.*, 2020], not only allow the model to focus more effectively on learning from tail data but also enhance its overall performance.

3 Methods

Cellular annotation is an important step in single-cell transcriptome analysis, which aims to infer the type, state, or function of each cell based on the gene expression profile of a single cell [Moffitt *et al.*, 2018; Brbić *et al.*, 2020]. Fundamentally, cellular annotation involves inferring cell types through the expression of specific marker genes [Cao *et al.*, 2020]. For example, CD3D/CD3E is used to label T cells, CD19 is used to label B cells, CD68 is used to label macrophages, and ACTA2 is used to label myofibroblasts. Through Differential Expressed Genes (DEG) analysis, genes that are highly specifically expressed in each cell subpopulation are found and annotated with known marker genes. For single-cell transcriptome analysis, dimensionality reduction (e.g., PCA, t-SNE, UMAP) and clustering (e.g., Louvain, Leiden’s algorithm) methods are commonly used to cluster cells with similar expression patterns into one group [Zhang *et al.*, 2019]. Differentially expressed genes in each cluster are analyzed and annotated in combination with marker genes and databases.

In order to cope with the high dimensionality and intricate relationships of mRNA data, we propose the Genomic Language Model (GLM) pre-training model, which is unsupervisedly trained on our constructed dataset to learn the rich gene interrelationships, and considering the long-tailed distribution of the data and the imbalance of the data, we incorporate the “GInf” loss function and HDM, and the details of the implementation are shown in the following sections.

3.1 Pretraining Process

We developed the GLM, which integrates data processing concepts from large language models [Zhang *et al.*, 2010; Goldberg, 2017; Amodio *et al.*, 2019] into its framework during the pretraining phase. Specifically, in single-cell transcriptomic data, each gene’s expression value represents its unique role in cellular function and state, akin to the semantic representation of tokens in language models. Consequently, we redefined the basic units of single-cell transcriptomic data as conceptual structures within a language model framework. Each gene expression value is treated as the smallest data unit, analogous to a token in language models—a fundamental unit with independent semantics. Furthermore, we conceptualize a cell, defined by the expression values of all its genes, as equivalent to a sentence in language models. In large language models, sentences are structural units composed of a series of tokens that convey contextual relationships and overall semantics. Similarly, in the GLM, cells are functional units formed by the combination of gene expression values, reflecting their intrinsic associations and overall functions.

We referenced the methods in scGPT [Cui *et al.*, 2023] and assigned a unique integer ID to each gene in the gene dictionary. This allows us to represent the gene expression profiles of each cell as a vector

$$Cg^{[i]} = [id(g_1^{[i]}), id(g_2^{[i]}), \dots] \quad (i \in \{1, \dots, n\}).$$

Here, g represents the gene, and i is the index of the gene. To avoid scale differences between different batches of data, we adopted a binning technique. We discretized the data from the same batch into continuous intervals $[b_k, b_{k+1}]$, where $k \in \{1, \dots, n\}$. Thus, different data points within the same interval were ultimately assigned the same integer value, effectively mitigating the impact of batch effects [Haghverdi *et al.*, 2018; Tran *et al.*, 2020] on model training.

Subsequently, we converted the gene names and gene expression values into emb_{gene} and emb_{value} through the traditional embedding layer. Here, emb_{gene} is analogous to the positional encoding information in large models. These embeddings, along with other conditional information, constitute the model’s input. The detailed data processing workflow is shown in Figure 2.

During the pre-training stage, we incorporated Transformer modules fortified with a multi-head attention mechanism to amplify the model’s proficiency in recognizing the interdependencies among distinct genes. Capitalizing on the widely-used unsupervised masked training scheme, we intentionally masked 15% of the gene expression values in a random fashion. Following this, we deployed a multilayer perceptron network to predict these obscured values. The optimization process served to further enhance the model’s efficacy, particularly through the application of the GInf loss function and repetitive training on samples that were misclassified with high confidence.

3.2 Long-Tailed Single-Cell Annotation

To better explore single-cell spatiotemporal omics, the most fundamental task is to annotate single cells. In the upstream unsupervised stage, the gene language model learns from massive unlabeled single-cell data via context masking, enabling accurate feature extraction from mRNA data. In the downstream task of cell annotation, the problem is transformed into a supervised data classification problem. However, due to the unique nature of diseases, even within diseased tissues or organs, the number of diseased cells is significantly smaller than the number of normal cells. Accurately annotating diseased cells, however, is critically important for related research. This long-tailed data distribution further increases the difficulty of cell annotation.

Traditional Definition: Cross-Entropy Loss

We denote the training set containing n samples as $D = \{\mathbf{x}_i, y_i\}$, where \mathbf{x}_i represents the i -th cell sample and y_i represents its corresponding annotation. For the definition of traditional tasks, this process can effectively be simplified into a classification deep learning task. the classifier of choice is the structurally simple VGG network [Tammina, 2019], where we only need to extract features using a well-trained single-cell GLM to extract the feature map of cell \mathbf{x}_i , and then input these features into a classifier represented by ψ to calculate

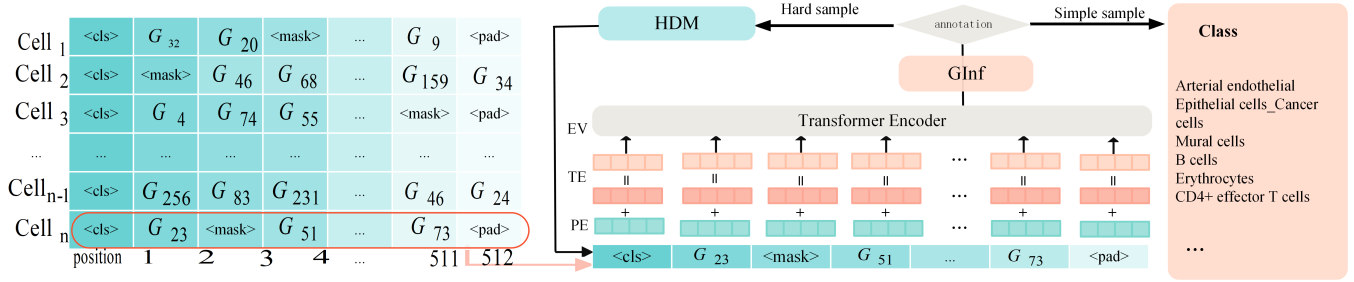


Figure 2: Schematic diagram of the model introduced structure, where PE is the Position Encoder, TE is the Token Embedding, and EV is the Embedding Vector.

the predicted logit of classifying \mathbf{x}_i into category j , as shown in the following Equation 1:

$$z_{ij} = \psi_j(\text{GLM}(x_i)). \quad (1)$$

The predicted probability of classifying \mathbf{x}_i into category j , with C denoting the total number of categories, is defined by passing the logit z_{ij} through a Softmax function, as shown in Equation 2:

$$\mathbf{p}_j(\mathbf{X}_i; \psi) = \frac{\exp(z_{ij})}{\sum_{l=1}^C \exp(z_{il})}. \quad (2)$$

Cross-entropy is commonly used as the loss function, as shown in Equation 3. However, this large language model approach based on the Cross-Entropy (CE) loss function [Cui *et al.*, 2023; Yang *et al.*, 2022; Wen *et al.*, 2023] tends to cause the model to focus a significant amount of attention on the head classes during training due to data imbalance issues. This results in overfitting of the head classes and underfitting of the tail classes, ultimately leading to suboptimal cell annotation results.

$$L_{\text{entropy}}(z_{ij}) = - \sum_{j=1}^c y_i \log(\mathbf{p}_j(\mathbf{X}_i; \psi)). \quad (3)$$

Gaussian Inflation Loss for Long-tail Distribution

Further, we consider that in human diseases, the number of diseased cells is relatively small compared to the number of normal cells, and even within the organs of affected individuals, diseased cells usually represent only a small fraction of the dataset. Since the cells of interest are located in the tails of the distribution, it is difficult for the network to focus on these tail categories, leading to a serious long-tail problem. To alleviate the above-mentioned problem, a feasible solution is to reduce the negative sample gradients imposed by head classes on tail classes. Therefore, we propose Gaussian Inflation Loss (GInf Loss) as a solution. By referring to and drawing inspiration from some reweighting methods [Li *et al.*, 2022; Wang *et al.*, 2021], we derive the GInf loss based on the CE loss as the fundamental paradigm, as shown in Equation 4.

$$\tilde{L}_{\text{GInf}}(z_{ij}) = - \sum_{j=1}^c y_i \log(\tilde{\mathbf{p}}_j(\mathbf{X}_i; \psi)). \quad (4)$$

The GInf loss is derived by optimizing the Softmax function and adjusting the hyperparameters N_j of different categories, forcing the network to pay more attention to tail categories and promoting their convergence. Additionally, the logit variable ψ predicted by the network is modified to z_{ij}^{inf} , as shown in Equation 5.

$$\tilde{\mathbf{p}}_j(\mathbf{X}_i; \psi) = \frac{N_j \exp(z_{ij}^{\text{inf}})}{\sum_{l \neq j}^c N_l \exp(z_{il}^{\text{inf}}) + N_j \exp(z_{ij}^{\text{inf}})}. \quad (5)$$

The soul of our method GInf Loss is z_{ij}^{inf} , which is Equation 6. To explain the underlying principle, we plot Figure 3. From the figure 3, it can be observed that in the feature space of logits, we aim to use a Gaussian distribution to enlarge the spatial proportion occupied by individual instances of tail categories, thereby balancing the overall proportion occupied by head categories in the feature space.

$$z_{ij}^{\text{inf}} = z_{ij} + \Delta\delta I. \quad (6)$$

where $I \sim \mathcal{N}(\mu, \Sigma)$ is infaction sample from Gaussian distribution and μ is the mean vector and Σ is the covariance matrix, $\Delta\delta$ is a parameter which is used to adjust the amplitude of inflation and we control it to a very small number. The relationship between the inflation factor and the decision boundary establishes the inflation factor related to the class.

$$\Delta\delta = \log N_{\text{max}} - \log N_j. \quad (7)$$

To keep the category inflation factor consistent, we set the inflation factor to be Equation 7. Here, N_j is the number of j classes frequent samples in the training set, the same as N_i .

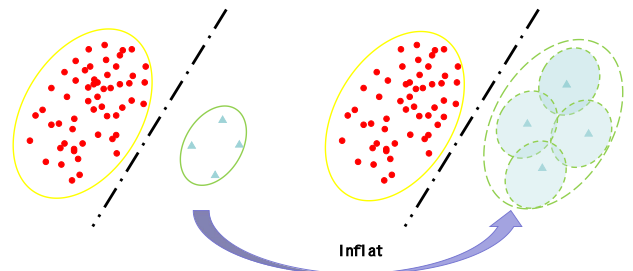


Figure 3: Gaussian Inflation Expands Tail Classes.

3.3 Hard Data Mining

When dealing with the problem of long-tailed data distributions, the introduction of the Gaussian expansion function provides some relief. However, the complexity of the long-tailed distribution problem inevitably requires more targeted strategies to further optimize model performance. To this end, we propose a method called Hard Data Mining (HDM). Unlike traditional training methods, HDM focuses on identifying and learning from sample categories critical to model performance but challenging to train. This approach allows the model to efficiently learn the feature distributions of challenging samples. In the HDM method, “hard samples” refer to categories that achieve high prediction scores in the model’s outputs, despite not being the true category of the current sample. These categories are often the most confusing for the model, as their scores are close to or sometimes even exceed those of the true category. This confusion reflects the current shortcomings of the model; therefore, focusing on these categories can significantly improve the model’s classification ability.

Specifically, HDM dynamically selects the hard-to-classify categories as training priorities by comparing the prediction scores output by the model, excluding the true category, and selecting the highest-scoring categories. Assuming there are C categories in total, the defined hard category set Ω_{ij} consists of hard samples for which the original class of \mathbf{x}_{ij} was j but were misclassified by the model into other categories. From the C misclassified categories, the top n hard samples with the highest logit scores in each category are selected to form the set. In this experiment, n is set to 20. This process not only enhances the model’s ability to distinguish between confusing categories, but also ensures more efficient use of training resources. By this design, HDM allows the model to focus more on challenging samples rather than simply optimizing the distribution of easily classified samples. This strategy proves to be particularly advantageous in complex and diverse tasks. The definition of the hard category set Ω_i can be expressed as follows: for any sample \mathbf{x}_i , the hard category set Ω_i composed of the selected categories can be expressed as (8).

$$\Omega_i = \bigcup_{l=1}^c \text{Top}_n \{x_{ij}, z_{il} \mid l \neq j\} \cup \{z_{ij}\}, \quad (8)$$

where Top_n means selecting C_{hard} examples with the largest values. In order to adapt better to long-tailed learning, we compute the probabilities of the selected categories in a balanced way,

$$L_{\text{GInf}}^{\text{hard}}(z_{ij}) = - \sum_{j=1}^c \log \left(\frac{N_j \exp(z_{ij}^{\text{inf}})}{\sum_{z_{il} \in \Omega_i} N_l \exp(z_{il})} \right), \quad (9)$$

where N_j represents the normalization term for category j . In the proposed GInf, this training strategy can be integrated into the previous process and executed synchronously.

$$L_{\text{GInf}}(z_{ij}) = \tilde{L}_{\text{GInf}}(z_{ij}) + L_{\text{GInf}}^{\text{hard}}(z_{ij}). \quad (10)$$

The total loss is ultimately expressed as the summation of GInf and the hard sample re-training terms.

4 Experiments

4.1 Dataset

Dataset	Celler-75	MS	hPancreas
Cell Num	41,307,753	13,468	10,600
Gene Num	21,292	3,000	3,000
Celltype	Full 20 Sub 45	18	13
Tissue	80	3	Pancreas-Only
Disease	75	Multiple Sclerosis	Pancreas-Related

Table 1: Comparison of datasets Celler-75, MS, and hPancreas.

Multiple Sclerosis (MS) and hPancreas dataset

The Multiple Sclerosis (MS) [Schirmer *et al.*, 2019] and hPancreas [Chen *et al.*, 2023] datasets are publicly accessible resources specifically designed for studying certain human diseases. The detail of these two public dataset was show in Table 1. The hPancreas dataset focuses on the study of the human pancreas. It contains a wealth of single-cell transcriptomic gene expression data, with 10,600 samples in the training set and 4,218 samples in the test set. These data are widely used in research on pancreatic-related disease mechanisms, the discovery of diagnostic biomarkers, and the development of therapeutic strategies.

On the other hand, the MS dataset is dedicated to the study of multiple sclerosis. This dataset includes multimodal data from both patients and healthy control groups, aimed at exploring the pathological mechanisms of the disease and identifying potential biomarkers. Specifically, the MS dataset consists of 13,468 training samples and 7,844 test samples, providing strong support for both basic research and clinical translation efforts in the field of multiple sclerosis.

Celler-75 dataset

Celler-75 is a high-dimensional single-cell dataset independently constructed by us, focusing on 75 specific human diseases across 70 major human organs, including major diseases such as cancer and Alzheimer’s disease. As shown in Table1, when compared with publicly available single-organ datasets like MS and hPancreas, Celler-75 demonstrates significant advantages due to its massive scale, which integrates over 40 million single-cell data points and more than 9 million gene expression profiles. The number of cells included in Celler-75 is approximately 3,000 times that of public datasets. Due to the increased scale of the dataset, we have refined the classification dimensions in the creation of cell annotation category labels, intentionally distinguishing between subclass and parent class levels. The specifics will be elaborated in the next section on metrics. Such a large-scale, high-quality single-cell dataset provides a solid foundation for the training and fine-tuning of large-scale gene models, significantly enhancing Celler’s performance in terms of cell type diversity and annotation accuracy. This dataset encompasses various types of cancers and other complex cellular pathological states, providing robust support for comprehensively analyzing the heterogeneity and specificity of disease-related gene expression at the cellular level. Additionally, the data distribution of 70 organ types and their proportions in the overall

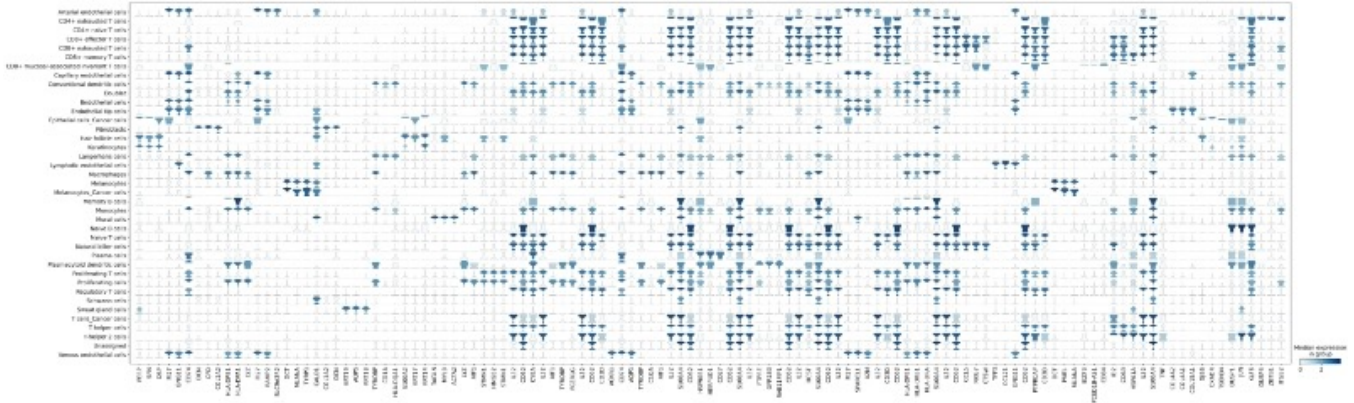


Figure 4: The bubble chart visualization illustrating gene expression levels and cell proportions.

Cell Type	New Column	SCBert			SCGpt			CellPLM			Celler		
		f1-score	precision	recall									
Brain	Parent-Classes	0.727±.012	0.705±.203	0.782±.007	0.919±.032	0.917±.063	0.921±.170	0.931±.002	0.935±.006	0.928±.002	0.956±.067	0.956±.032	0.957±.003
	Subclasses	0.787±.011	0.789±.239	0.806±.025	0.802±.036	0.827±.041	0.777±.104	0.779±.126	0.794±.081	0.765±.037	0.890±.026	0.886±.051	0.895±.113
kidney	Parent-Classes	0.841±.023	0.823±.039	0.805±.024	0.880±.017	0.885±.048	0.875±.021	0.881±.005	0.888±.016	0.874±.012	0.820±.019	0.805±.004	0.835±.016
	Subclasses	0.668±.005	0.704±.022	0.665±.031	0.679±.040	0.712±.018	0.648±.004	0.695±.018	0.717±.124	0.673±.106	0.879±.034	0.890±.041	0.869±.025
liver	Parent-Classes	0.636±.107	0.712±.111	0.626±.042	0.906±.019	0.914±.008	0.898±.030	0.885±.017	0.886±.042	0.884±.014	0.969±.008	0.964±.021	0.975±.021
	Subclasses	0.618±.031	0.628±.004	0.641±.021	0.789±.067	0.806±.034	0.773±.029	0.759±.038	0.785±.033	0.735±.029	0.840±.024	0.868±.016	0.813±.015
Skin	Parent-Classes	0.690±.016	0.780±.011	0.660±.019	0.875±.034	0.879±.028	0.870±.019	0.875±.007	0.877±.009	0.874±.011	0.870±.015	0.868±.017	0.873±.011
	Subclasses	0.676±.012	0.674±.009	0.724±.023	0.630±.043	0.666±.028	0.596±.030	0.685±.024	0.706±.018	0.666±.014	0.860±.024	0.862±.031	0.859±.035

Table 2: Performance comparison between Celler and other advanced approaches (i.e., SCBert, SCGpt, CellPLM) across different tissues (i.e., brain, kidney, liver, skin).

dataset are visualized in Supplementary Figure 1. Furthermore, the category information of 75 diseases is listed individually in Supplementary Table 1.

4.2 Metric

In single-cell transcriptomics studies, the classification of cell types typically includes Parent Classes and Subclasses, which together form a hierarchical structure of cell categorization. In our private dataset, Cell-75, biologically meaningful labels for both the Parent Class and Subclass levels are provided. Parent Classes refer to groups of cells with similar functions or shared developmental origins, and these categories are defined based on global gene expression characteristics. Subclasses, on the other hand, are more specific manifestations of Parent Classes, representing finer-grained cell types or states with distinct functional characteristics and expression of marker genes. For example, under the Parent Class of immune cells, Subclasses may include T cells, B cells, and natural killer (NK) cells. Thus, if a cell is identified as a T cell, its Parent Class label would be immune cells, and its Subclass label would be T cells.

Accurately annotating cell types across this hierarchical structure is critical for understanding cellular diversity and functional heterogeneity. To achieve this, robust evaluation metrics are required to assess how well the predicted annotations align with the true cell types. Here, we employ three key metrics to evaluate the performance of cell annotation methods: *F1 Score*: Balances Precision and Recall, serving as a comprehensive evaluation metric for cell annotation per-

formance by finding a trade-off between annotation accuracy and coverage. *Precision*: the accuracy of predicting specific cell types (e.g., immune cells) by minimizing false positives, ensuring cells are not incorrectly labeled. *Recall*: measures the ability to correctly identify cells belonging to a particular type by reducing false negatives, which is especially important for annotating rare cell types.

4.3 Evaluation

Cell Annotation Performance on Cell-75

In the horizontal comparison experiments, we selected three SOTA methods published in the journal *Nature Methods* as comparative experiments, including CellPLM [Wen *et al.*, 2023], scBERT [Yang *et al.*, 2022], and scGPT [Cui *et al.*, 2023]. The experimental results are presented in Table 2. The training dataset for the comparison experiments was sourced from four organs—liver, kidney, skin, and brain. Each cell type was assessed at two levels of granularity: Parent-Classes and Subclasses. The dataset contains a total of 800,000 samples, with 600,000 used for fine-tuning and 200,000 for testing. The distribution of cell categories in the test data for each organ is as follows: Brain: 52 subclasses, 32 parent classes; Skin: 47 subclasses, 21 parent classes; Liver: 48 subclasses, 24 parent classes; Kidney: 59 subclasses, 32 parent classes. The experimental results indicate that the classification performance of Parent-Classes is generally better than that of Subclasses, suggesting that finer-grained subclass classification tasks pose greater challenges to the algorithms. As shown in Table 2, the Celler method demonstrates signif-

icant advantages in the *F1-score*, *precision*, and *recall* metrics, with its performance indicators (values marked in red) generally surpassing other methods. The second-best results are marked in blue. However, in certain scenarios (e.g., the Parent-Class classification tasks for Kidney and Skin), the performance of the Celler method shows some fluctuations.

Cell Annotation Performance on Open Access Dataset

Method	MS		hPancreas	
	F1 (\uparrow)	Precision (\uparrow)	F1 (\uparrow)	Precision (\uparrow)
CellTypist	0.667 \pm .002	0.693 \pm .001	0.708 \pm .023	0.736 \pm .025
ACTINN	0.628 \pm .012	0.634 \pm .009	0.705 \pm .005	0.709 \pm .006
SingleCellNet	0.637 \pm .001	0.700 \pm .001	0.739 \pm .006	0.761 \pm .004
TOSICA*	0.578	0.664	0.656	0.661
scBERT	0.599 \pm .001	0.604 \pm .004	0.685 \pm .003	0.699 \pm .007
scGPT	0.703 \pm .002	0.729 \pm .002	0.718 \pm .003	0.735 \pm .001
<i>Celler</i>	0.799 \pm .004	0.841 \pm .002	0.767 \pm .010	0.755 \pm .010

Table 3: **The results of cell type annotation on the MS and hPancreas datasets.** * indicates results directly taken from CellPLM.

We follow the suggestion of CellPLM [Wen *et al.*, 2023] and GenePT [Chen and Zou, 2023] to include hPancreas [Chen *et al.*, 2023] and Multiple Sclerosis (MS) [Schirmer *et al.*, 2019] datasets. As can be seen in table 3, Celler outperforms CellTypist [Domínguez Conde *et al.*, 2022], ACTINN [Ma and Pellegrini, 2020], SingleCellNet [Tan and Cahan, 2019], TOSICA [Chen *et al.*, 2023], scBERT [Yang *et al.*, 2022], and scGPT [Cui *et al.*, 2023], achieving the highest performance on both the MS and hPancreas datasets, demonstrating its superiority in classification tasks. In comparison, SingleCellNet achieves a Precision of 0.761 ± 0.004 on the hPancreas dataset, ranking closely behind, but its overall F1 score is still lower than Celler. ScGPT performs well on the MS dataset. Other methods, such as CellTypist and ACTINN, show moderate performance, while TOSICA produces less satisfactory results on both datasets. In summary, Celler demonstrates stronger robustness and accuracy in handling these tasks. These results indicate that, Celler is able to identify the underlying features of gene expression patterns as well as remote gene-gene dependencies, and achieve a comprehensive high-level representation of cell type-specific global information.

4.4 Variation in Gene Expression Characteristics across Cell Types.

Figure 4 illustrates the expression patterns of different genes (horizontal axis) across various cell types (vertical axis), as well as the significance and breadth of their expression. Gene expression levels are represented by the size and color intensity of the bubbles. In immune cells, such as T cells and macrophages, certain genes show prominent expression. For example, CD3D, CD3E, CD4, and HLA-DRB1 are significantly expressed in CD4+ T cells (e.g., CD4+ exhausted T cells and CD4+ naive T cells), while CD8A and CD8B are specifically expressed in CD8+ T cells. Likewise, genes such as CD68 and HLA-DRB1 show high expression levels in macrophages. In endothelial cells (e.g., arterial and capillary

endothelial cells), CDH5 and VWF serve as signature genes, indicating their close association with angiogenesis and vascular maintenance. In epithelial and cancer cells, KRT19 and KRT7 are highly expressed, reflecting epithelial cell characteristics and tumor-related expression changes. In stem cells (e.g., Stem/B cells), PROM1 and SOX2 are closely linked to proliferation and differentiation functions. Unassigned or undifferentiated cells exhibit lower expression levels for certain genes, while specific cell types, such as keratinocytes and Langerhans cells, show distinct markers like KRT14/KRT5 and CD207, highlighting their unique biological functions.

4.5 Ablation Experiments

Methods	Precision	Recall	F1-score
CE Loss	0.910 \pm .004	0.826 \pm .006	0.797 \pm .007
Focal Loss	0.919 \pm .007	0.862 \pm .009	0.821 \pm .011
Ride Loss	0.921 \pm .005	0.851 \pm .009	0.877 \pm .010
Ours	0.951 \pm .003	0.886 \pm .012	0.895 \pm .009

Table 4: Ablation study on different loss functions.

To validate the effectiveness of our proposed expansion loss on long-tailed datasets, we conducted an ablation study on a human brain disease dataset. The experiment compared our method with well-known long-tailed loss functions (e.g., Focal Loss [Lin, 2017] and RIDE Loss [Kumar *et al.*, 2021]) as well as the traditional cross-entropy loss (CE Loss) [Mao *et al.*, 2023] from that does not consider long-tailed distributions. The results demonstrate that our method achieved significant improvements across multiple metrics, particularly in balancing precision and recall with the F1-score, showing an increase of nearly 10% compared to CE Loss. This strongly validates the superior performance of our method in handling classification tasks on long-tailed distributions. Detailed results are presented in the Table 4.

5 Conclusion

Our research results show that Celler performs extremely well when facing the public datasets MS, hPancreas, and our large-scale private dataset Celler-75. It improves the accuracy of identifying rare cell types by over 10% compared with the scBert model, and its overall F1 Score is also significantly better than other benchmark models, highlighting its excellent generalization capability and practical application value. Efficient single-cell data annotation is of great significance for disease diagnosis, personalized medicine, and the discovery of biomarkers. The introduction of Celler not only breaks the limitations of existing annotation methods in handling long-tail distribution data but also provides strong tool support for the integrated analysis of complex multi-omics data in the future.

Acknowledgments

This research received generous support from the National Natural Science Foundation of China (Grant No. 62076092) pertaining to the project titled "Intelligent Speech Dialogue System Response Generation for Affective Computing" spanning the duration 2021-2024.

References

- [Amodio *et al.*, 2019] Matthew Amodio, David Van Dijk, Krishnan Srinivasan, William S Chen, Hussein Mohsen, Kevin R Moon, Allison Campbell, Yujiao Zhao, Xiaomei Wang, Manjunatha Venkataswamy, et al. Exploring single-cell data with deep multitasking neural networks. *Nature methods*, 16:1139–1145, 2019.
- [Brbić *et al.*, 2020] Maria Brbić, Marinka Zitnik, Sheng Wang, Angela O Pisco, Russ B Altman, Spyros Darnanis, and Jure Leskovec. Mars: discovering novel cell types across heterogeneous single-cell experiments. *Nature methods*, 17(12):1200–1206, 2020.
- [Buda *et al.*, 2018] Mateusz Buda, Atsuto Maki, and Maciej A Mazurowski. A systematic study of the class imbalance problem in convolutional neural networks. *Neural networks*, 106:249–259, 2018.
- [Cao *et al.*, 2019] Junyue Cao, Malte Spielmann, Xiaojie Qiu, Xingfan Huang, Daniel M Ibrahim, Andrew J Hill, Fan Zhang, Stefan Mundlos, Lena Christiansen, Frank J Steemers, et al. The single-cell transcriptional landscape of mammalian organogenesis. *Nature*, 566(7745):496–502, 2019.
- [Cao *et al.*, 2020] Yinghao Cao, Xiaoyue Wang, and Gongxin Peng. Scsa: a cell type annotation tool for single-cell rna-seq data. *Frontiers in genetics*, 11:490, 2020.
- [Chawla *et al.*, 2002] Nitesh V Chawla, Kevin W Bowyer, Lawrence O Hall, and W Philip Kegelmeyer. Smote: synthetic minority over-sampling technique. *Journal of artificial intelligence research*, 16:321–357, 2002.
- [Chen and Zou, 2023] Yiqun Chen and James Zou. Genept: A simple but effective foundation model for genes and cells built from chatgpt. *bioRxiv*, 2023. Preprint.
- [Chen *et al.*, 2023] Jiawei Chen, Hao Xu, Wanyu Tao, Zhaoxiong Chen, Yuxuan Zhao, and Jing-Dong J Han. Transformer for one stop interpretable cell type annotation. *Nature Communications*, 14(1):223, 2023.
- [Cui *et al.*, 2023] Haotian Cui, Chloe Wang, Hassaan Maan, and Bo Wang. scgpt: Towards building a foundation model for single-cell multi-omics using generative ai. *bioRxiv*, pages 2023–04, 2023.
- [Domínguez Conde *et al.*, 2022] C Domínguez Conde, LB Xu, DB Jarvis, DB Rainbow, SB Wells, T Gomes, SK Howlett, O Suchanek, K Polanski, HW King, et al. Cross-tissue immune cell analysis reveals tissue-specific features in humans. *Science*, 376(6594):eabl5197, 2022.
- [Ganin and Lempitsky, 2015] Yaroslav Ganin and Victor Lempitsky. Unsupervised domain adaptation by backpropagation. In *International conference on machine learning*, pages 1180–1189. PMLR, 2015.
- [Goldberg, 2017] Yoav Goldberg. *Neural Network Methods for Natural Language Processing*, volume 10. Springer, 2017.
- [Gong *et al.*, 2023] Jing Gong, Minsheng Hao, Xingyi Cheng, Xin Zeng, Chiming Liu, Jianzhu Ma, Xuegong Zhang, Taifeng Wang, and Le Song. xtrimogene: An efficient and scalable representation learner for single-cell rna-seq data. *Advances in Neural Information Processing Systems*, 15(3):123–135, 2023.
- [Grabski and Irizarry, 2022] Isabella N Grabski and Rafael A Irizarry. A probabilistic gene expression barcode for annotation of cell types from single-cell rna-seq data. *Biostatistics*, 23(4):1150–1164, 2022.
- [Haghverdi *et al.*, 2018] Laleh Haghverdi, Aaron TL Lun, Michael D Morgan, and John C Marioni. Batch effects in single-cell rna-sequencing data are corrected by matching mutual nearest neighbors. *Nature biotechnology*, 36(5):421–427, 2018.
- [He and Garcia, 2009] Haibo He and Edwardo A Garcia. Learning from imbalanced data. *IEEE Transactions on knowledge and data engineering*, 21(9):1263–1284, 2009.
- [He *et al.*, 2020] Shuai He, Lin-He Wang, Yang Liu, Yi-Qi Li, Hai-Tian Chen, Jing-Hong Xu, Wan Peng, Guo-Wang Lin, Pan-Pan Wei, Bo Li, et al. Single-cell transcriptome profiling of an adult human cell atlas of 15 major organs. *Genome biology*, 21:1–34, 2020.
- [Huang *et al.*, 2021] Qianhui Huang, Yu Liu, Yuheng Du, and Lana X Garmire. Evaluation of cell type annotation r packages on single-cell rna-seq data. *Genomics, Proteomics and Bioinformatics*, 19(2):267–281, 2021.
- [Kumar *et al.*, 2021] R. Kumar, S. Liu, Z. Tian, Z. Zhong, and J. Jia. A2-ride: Long-tailed recognition by routing diverse and enhanced experts. *arXiv preprint arXiv:2101.10633*, 2021.
- [Li *et al.*, 2022] Mengke Li, Yiu-ming Cheung, and Yang Lu. Long-tailed visual recognition via gaussian clouded logit adjustment. In *Proceedings of the IEEE/CVF Conference on Computer Vision and Pattern Recognition*, pages 6929–6938, 2022.
- [Lin, 2017] Tsung-Yi Lin. Focal loss for dense object detection. *arXiv preprint arXiv:1708.02002*, 2017.
- [Lukassen *et al.*, 2020] Soeren Lukassen, Robert Lorenz Chua, Timo Trefzer, Nicolas C Kahn, Marc A Schneider, Thomas Muley, Hauke Winter, Michael Meister, Carmen Veith, Agnes W Boots, et al. Sars-cov-2 receptor ace2 and tmprss2 are primarily expressed in bronchial transient secretory cells. *The EMBO journal*, 39:e105114, 2020.
- [Ma and Pellegrini, 2020] Feiyang Ma and Matteo Pellegrini. Actinn: automated identification of cell types in single cell rna sequencing. *Bioinformatics*, 36(2):533–538, 2020.
- [Mao *et al.*, 2023] Anqi Mao, Mehryar Mohri, and Yutao Zhong. Cross-entropy loss functions: Theoretical analysis and applications. In Andreas Krause, Emma Brunskill, Kyunghyun Cho, Barbara Engelhardt, Sivan Sabato, and Jonathan Scarlett, editors, *Proceedings of the 40th International Conference on Machine Learning*, volume 202 of *Proceedings of Machine Learning Research*, pages 23803–23828. PMLR, 23–29 Jul 2023.

- [McDavid *et al.*, 2013] Andrew McDavid, Greg Finak, Pratip K Chattopadhyay, Maria Dominguez, Laurie Lamoreaux, Steven S Ma, Mario Roederer, and Raphael Gottardo. Data exploration, quality control and testing in single-cell qpcr-based gene expression experiments. *Bioinformatics*, 29:461–467, 2013.
- [Moffitt *et al.*, 2018] Jeffrey R Moffitt, Dhananjay Bambah-Mukku, Stephen W Eichhorn, Eric Vaughn, Karthik Shekhar, Julio D Perez, Nimrod D Rubinstein, Junjie Hao, Aviv Regev, Catherine Dulac, et al. Molecular, spatial, and functional single-cell profiling of the hypothalamic preoptic region. *Science*, 362:au5324, 2018.
- [Pasquini *et al.*, 2021] Giovanni Pasquini, Jesus Eduardo Rojo Arias, Patrick Schäfer, and Volker Busskamp. Automated methods for cell type annotation on scrna-seq data. *Comput. Struct. Biotechnol. J.*, 19:961–969, 2021.
- [Plass *et al.*, 2018] Mireya Plass, Jordi Solana, F Alexander Wolf, Salah Ayoub, Aristotelis Misios, Petar Glažar, Benedikt Obermayer, Fabian J Theis, Christine Kocks, and Nikolaus Rajewsky. Cell type atlas and lineage tree of a whole complex animal by single-cell transcriptomics. *Science*, 360(6391):eaq1723, 2018.
- [Pliner *et al.*, 2019] Hannah A Pliner, Jay Shendure, and Cole Trapnell. Supervised classification enables rapid annotation of cell atlases. *Nature methods*, 16:983–986, 2019.
- [Schaum *et al.*, 2018] Nicholas Schaum, Jim Karknias, Norma F Neff, Andrew P May, Stephen R Quake, Tony Wyss-Coray, Spyros Darmanis, Joshua Batson, Olga Botvinnik, Michelle B Chen, et al. Single-cell transcriptomics of 20 mouse organs creates a tabula muris. *Nature*, 562(7727):367, 2018.
- [Schirmer *et al.*, 2019] Lucas Schirmer, Dmitry Velmeshev, Staffan Holmqvist, Max Kaufmann, Sebastian Werneburg, Diane Jung, Stephanie Vistnes, John H Stockley, Adam Young, Maike Steindel, et al. Neuronal vulnerability and multilineage diversity in multiple sclerosis. *Nature*, 573(7772):75–82, 2019.
- [Shen *et al.*, 2023] Hongru Shen, Jilei Liu, Jiani Hu, Xilin Shen, Chao Zhang, Dan Wu, Mengyao Feng, Meng Yang, Yang Li, Yichen Yang, et al. Generative pretraining from large-scale transcriptomes for single-cell deciphering. *IScience*, 26(5), 2023.
- [Tammina, 2019] Srikanth Tammina. Transfer learning using vgg-16 with deep convolutional neural network for classifying images. *International Journal of Scientific and Research Publications (IJSRP)*, 9(10):143–150, 2019.
- [Tan and Cahan, 2019] Yuqi Tan and Patrick Cahan. Single-cellnet: a computational tool to classify single cell rna-seq data across platforms and across species. *Cell Systems*, 9(2):207–213, 2019.
- [Tarashansky *et al.*, 2021] Alexander J Tarashansky, Jacob M Musser, Margarita Khariton, Pengyang Li, Detlev Arendt, Stephen R Quake, and Bo Wang. Mapping single-cell atlases throughout metazoa unravels cell type evolution. *eLife*, 10:e66747, 2021.
- [Theodoris *et al.*, 2023] Christina V Theodoris, Ling Xiao, Anant Chopra, Mark D Chaffin, Zeina R Al Sayed, Matthew C Hill, Helene Mantineo, Elizabeth M Brydon, Zexian Zeng, X Shirley Liu, et al. Transfer learning enables predictions in network biology. *Nature*, 618:616–622, 2023.
- [Tran *et al.*, 2020] Hoa Thi Nhu Tran, Kok Siong Ang, Marion Chevrier, Xiaomeng Zhang, Nicole Yee Shin Lee, Michelle Goh, and Jinmiao Chen. A benchmark of batch-effect correction methods for single-cell rna sequencing data. *Genome biology*, 21:12, 2020.
- [Wang *et al.*, 2021] Jiaqi Wang, Wenwei Zhang, Yuhang Zang, Yuhang Cao, Jiangmiao Pang, Tao Gong, Kai Chen, Ziwei Liu, Chen Change Loy, and Dahua Lin. Seesaw loss for long-tailed instance segmentation. In *Proceedings of the IEEE/CVF conference on computer vision and pattern recognition*, pages 9695–9704, 2021.
- [Wen *et al.*, 2023] Hongzhi Wen, Wenzhuo Tang, Xinnan Dai, Jiayuan Ding, Wei Jin, Yuying Xie, and Jiliang Tang. Cellplm: pre-training of cell language model beyond single cells. *bioRxiv*, pages 2023–10, 2023.
- [Yang *et al.*, 2022] Fan Yang, Wenchuan Wang, Fang Wang, Yuan Fang, Duyu Tang, Junzhou Huang, Hui Lu, and Jianhua Yao. scbert as a large-scale pretrained deep language model for cell type annotation of single-cell rna-seq data. *Nature Machine Intelligence*, 4(10):852–866, 2022.
- [Zhang *et al.*, 2010] Yin Zhang, Rong Jin, and Zhi-Hua Zhou. Understanding bag-of-words model: a statistical framework. *International journal of machine learning and cybernetics*, 1:43–52, 2010.
- [Zhang *et al.*, 2019] Ze Zhang, Danni Luo, Xue Zhong, Jin Huk Choi, Yuanqing Ma, Stacy Wang, Elena Mahrt, Wei Guo, Eric W Stawiski, Zora Modrusan, et al. Scina: a semi-supervised subtyping algorithm of single cells and bulk samples. *Genes*, 10:531, 2019.
- [Zhang *et al.*, 2020] Y. Zhang, Y. Chen, and L. Li. Impacts of ride-hailing on energy and the environment: a systematic review. *Transportation Research Part D: Transport and Environment*, 85:102401, 2020.
- [Zhao *et al.*, 2020] Xinlei Zhao, Shuang Wu, Nan Fang, Xiao Sun, and Jue Fan. Evaluation of single-cell classifiers for single-cell rna sequencing data sets. *Briefings in bioinformatics*, 21(5):1581–1595, 2020.
- [Zhong *et al.*, 2016] Qiaoyong Zhong, Chao Li, Yingying Zhang, H Sun, S Yang, D Xie, and S Pu. Towards good practices for recognition & detection. In *CVPR workshops*, volume 1, page 3, 2016.
- [Zhou *et al.*, 2020] Boyan Zhou, Quan Cui, Xiu-Shen Wei, and Zhao-Min Chen. Bbn: Bilateral-branch network with cumulative learning for long-tailed visual recognition. *arXiv preprint arXiv:1912.02413*, pages 9719–9728, 2020.